

# **Development of Hybrid Energy Harvester for Self-Powered Environmental Sensor**

by

Syafiq Bin Shahrizal

18168

Dissertation submitted in partial fulfilment of  
the requirements for the  
Bachelor of Engineering (Hons)  
(Electrical and Electronics Engineering)

JANUARY 2017

Universiti Teknologi PETRONAS  
32610 Bandar Seri Iskandar  
Perak Darul Ridzuan

CERTIFICATION OF APPROVAL

**Development of Hybrid Energy Harvester for Self-Powered Environmental Sensor**

by

Syafiq Bin Shaharizal

18168

A project dissertation submitted to the  
Electrical and Electronics Engineering Programme  
Universiti Teknologi PETRONAS  
in partial fulfillment of the requirement for the  
BACHELOR OF ENGINEERING (Hons)  
(ELECTRICAL AND ELECTRONICS ENGINEERING)

Approved by,

---

(Dr. Mohamad Radzi Bin Ahmad)

UNIVERSITI TEKNOLOGI PETRONAS  
BANDAR SERI ISKANDAR, PERAK

January 2017

## CERTIFICATION OF ORIGINALITY

This is to certify that I am responsible for the work submitted in this project, that the original work is my own except as specified in the references and acknowledgements, and that the original work contained herein have not been undertaken or done by unspecified sources or persons.

---

SYAFIQ BIN SHAHARIZAL

## **ABSTRACT**

The purpose of this research is to come out with a new type of energy harvester which is capable to produce higher output power as compared to the conventional energy harvester. This new model is known as hybrid energy harvester as it has both Piezoelectric and Magnetostrictive energy harvesters. The conventional energy harvester has some limitations i.e. it produces smaller output power and not quite sufficient to power up the low powered electronic devices, plus some of them only works in certain range of frequencies. With more than one energy harvesters are integrated, we can cover wider range of frequencies and able to increase the output power of this harvester. To construct the hybrid energy harvester, a mathematical model is first develop, then a simulation is carried out with MATLAB/Simulink. Circuit design and the prototype device are designed next. The mathematical model shows the basic concept of energy conversion from mechanical to electrical which is later simulated with MATLAB/Simulink. The results are analyzed and later to be compared with the actual prototype of the hybrid energy harvester. The hybrid energy harvester outputs AC power thus a rectifying circuit will be designed to produce a clean DC power. By introducing a power management circuit, we can power up low-powered devices such as environmental sensor or small electronic devices.

## **ACKNOWLEDGEMENT**

This work would not be possible without the support from my family. I would love to thank my parents, Mr. Shaharizal Mohd Shariff and Mrs. Normala Samsudin for all the encouragement and for being my ultimate role models. I would also like to express my deepest gratitude to Electrical and Electronic Engineering Department for giving me the opportunity to gain knowledge from this project and for all the resources throughout this project.

I would like to thank my supervisor, Dr. Mohamad Radzi Bin Ahmad for his patience and generosity with me from the start of the project until it reached its completion. Throughout the project with him, I have gain numerous knowledge on engineering aspect especially in energy harvesting. His knowledge wise brought a huge impact to my project and personal development. In addition, I would like to thank Electrical and Electronic Lab technician, Mr. Isnani for helping and guiding me with the PCB circuit design.

Finally, I am grateful to have friends who are always supporting me during good and difficult times. All the hardships that I have been through will only make me stronger. Thank you all.

# TABLE OF CONTENTS

<b>CERTIFICATION OF APPROVAL</b>	<b>ii</b>
<b>CERTIFICATION OF ORIGINALITY</b>	<b>iii</b>
<b>ABSTRACT</b>	<b>iv</b>
<b>ACKNOWLEDGEMENT</b>	<b>v</b>
<b>LIST OF FIGURES</b>	<b>viii</b>
<b>LIST OF TABLES</b>	<b>x</b>
<b>CHAPTER 1: INTRODUCTION</b>	<b>1</b>
1.1 Background	1
1.2 Problem Statement	2
1.3 Objective	3
1.4 Scope of Study	3
<b>CHAPTER 2: LITERATURE REVIEW</b>	<b>4</b>
2.1 Introduction	4
2.2 Piezoelectric Mechanism	4
2.3 Magnetostrictive Mechanism	6
2.4 Hybrid Energy Harvesting	7
<b>CHAPTER 3: METHODOLOGY</b>	<b>9</b>
3.1 Gantt chart	10
3.2 Project Milestone	12
3.3 Mathematical Model	13
3.4 Simulink Block	15

3.5	Table of Parameters	16
3.6	Designing Power Management Circuit	17
3.7	Components Selection for PCB design	18
3.8	Power Management Circuit	19
	3.8.1 Schematic Design	19
	3.8.2 Board Layout	20
	3.8.3 Board Adjustment	21
	3.8.4 Fabricated PCB	22
3.9	Prototype Design Piezoelectric Energy Harvester	23
3.10	Prototype Design Electromagnetic Energy Harvester	24
<b>CHAPTER 4:</b>	<b>RESULTS AND DISCUSSION</b>	<b>27</b>
4.1	Output Voltage of Piezoelectric	27
4.2	Output Voltage of Magnetostrictive	29
4.3	Experimenting on Hybrid Energy Harvester	31
	4.3.1 Resonance Frequency of Electromagnetic Energy Harvester	33
	4.3.2 Resonance Frequency of Piezoelectric Energy Harvester	36
<b>CHAPTER 5:</b>	<b>CONCLUSION AND RECOMMENDATION</b>	<b>37</b>
5.1	Conclusion	37
5.2	Recommendation	38
	<b>REFERENCES</b>	<b>39</b>
	<b>APPENDICES</b>	<b>41</b>

## LIST OF FIGURES

Figure 2.1	Piezoelectric Bimorph Cantilever Mechanism	5
Figure 2.2	Mass, spring and damper model for Piezoelectric Energy Harvester	6
Figure 2.3	Magnetostrictive Cantilever Mechanism	7
Figure 2.4	Block diagram representing the Energy Harvesting Module	8
Figure 3.1	Gantt chart for FYP 1	10
Figure 3.2	Gantt chart for FYP 2	11
Figure 3.3	Project Milestone	12
Figure 3.4	Simulink Block of the Hybrid Energy Harvester	15
Figure 3.5	Schematic for Power Management Circuit	19
Figure 3.6	Equivalent Board for Power Management Circuit	20
Figure 3.7	Modified Board	21
Figure 3.8	Completed PCB Board	22
Figure 3.9	Side View	23
Figure 3.10	Top Side View	23
Figure 3.11	Side View	24
Figure 3.12	Top Side View	25
Figure 3.13	Hybrid Energy Harvester Prototype which consist of Piezoelectric and Electromagnetic Harvester.	25
Figure 3.14	Completed Hybrid Energy Harvester	26
Figure 4.1	Input vibration that is applied to Piezoelectric	19
Figure 4.2	Output voltage of Piezoelectric	20
Figure 4.3	Voltage vs frequency in Piezoelectric	20
Figure 4.4	Input vibration that is applied to Magnetostrictive	21
Figure 4.5	Output voltage of Magnetostrictive	22
Figure 4.6	Voltage vs frequency in Magnetostrictive	22
Figure 4.7	Equipment setup in the vibration lab.	31



Figure 4.8	Hybrid Energy Harvester on Vibration Shaker	31
Figure 4.9	Voltage vs frequency in Coil 1	33
Figure 4.10	Voltage vs frequency in Coil 2	34
Figure 4.11	Voltage vs frequency in when Coil 1 and Coil 2 are connected in series	35
Figure 4.12	Voltage vs frequency in Piezoelectric	36

## LIST OF TABLES

Table 3.1	Simulation parameters for Piezoelectric	16
Table 3.2	Simulation parameters for Magnetostrictive	16
Table 3.3	Components on the PCB	18
Table 4.1	Experiment parameters for Piezoelectric	32
Table 4.2	Experiment parameters for Electromagnetic	32

# CHAPTER 1

## INTRODUCTION

### 1.1 Background

Energy has become the most important factor in human civilization. One can't survive a day without energy source and the demand of energy has been growing drastically by years. With the depletion of non-renewable energy sources and instability of oil and gas industry, people have shown a lot of interest in developing devices to tap the natural environment energy sources such as solar, wind, tide and other ambient energies. Recently ambient energy has become famous among researches as it can be obtained easily from the surrounding and can be utilized to power up small devices which requires only small amount of energy. One of the common ambient energy sources is natural vibration such as the vibration of building structures, the movement of vehicles and also human motion [1]. These vibrations produces kinetic energy which need to be converted into electrical energy in order to power small electronic devices. This method is called Energy Harvesting.

To convert the vibration into electrical energy, a conversion mechanism is utilized. Among the conversion mechanisms used are Piezoelectric, Magnetostrictive, Electromagnetic and Radio-Frequency methods [2]. However, these conversion mechanisms produced small and non-continuous power supply [3, 4]. In order to meet the power requirement for most low powered devices, a hybrid energy harvester is introduced and explored. The proposed hybrid energy harvester is a combination of two conversion mechanism namely Piezoelectric and Magnetostrictive methods. Both conversion mechanisms are to be integrated into one system to maximize the output power.

## 1.2 Problem Statement

Even though the electrical energy can be obtained by any types of conversion mechanism, the power output produced by such mechanism is relatively small and insufficient to power miniaturized electronic devices. Conventional transduction mechanisms produced limited amount of power, depending on their reactions towards the vibration level. In other words, the individual mechanism can only capture specific range of frequencies depending on their conversion design. It has been found that this individual conversion mechanism is not sufficient to meet the power requirement of low-powered devices such as the wireless sensor.

To overcome this problem, a new type of energy harvesting is proposed to improve the conventional design. The proposed model is the combination of two conversion mechanisms namely Piezoelectric and Magnetostrictive methods. This new method is called Hybrid Energy Harvesting as both are converting the vibration energy separately but integrated into one device. The electrical energy produced is then fed into power conditioning units. In other words, both output are integrated into one system. Based on this model, the range of frequencies covered is expected to be larger than the individual converting mechanism, thus higher power output is produced. Moreover, the hybrid energy harvester is targeted to provide continuous output even though the magnitude and frequencies of the vibration source varies.

### **1.3 Objectives**

The objectives of this research are as follows;

- i. To investigate the possibility of integrating both the piezoelectric and magnetostrictive devices into a single device.
- ii. To develop the mathematical model and simulation of the hybrid energy harvester.
- iii. To investigate the effects of different frequencies range for each module of the energy harvester

### **1.4 Scope of Study**

The scope of study consists of three courses learned throughout the studies in Universiti Teknologi Petronas (UTP). The first part is the control system theory. The concept of mechanical block which consist of mass, spring and damper which represents the kinetic energy from ambient vibration. The mechanical block is then converted into equivalent electrical model and circuit to analyze the power conversion.

The second part involved analogue electronic theory in designing power management circuit. The alternating current (AC) is converted to a clean direct current (DC) output. The third part is the simulation of block diagram which representing the mechanical and electrical energy using the MATLAB/Simulink tool.

## **CHAPTER 2**

### **LITERATURE REVIEW**

#### **2.1 Introduction**

This chapter elaborates the individual converting mechanism, i.e. Piezoelectric and Magnetostrictive. The conversion principle of vibration energy to electrical energy will be explained in details. The combination of both mechanisms create a hybrid energy harvesting device.

#### **2.2 Piezoelectric Mechanism**

There are many types of Piezoelectric materials available but the most famous and commonly used nowadays are PZT material [5]. PZT stands for the Plumbum (Pb), Zirconate (Zr) and Titanate (Ti) elements which combines to form a crystal structure. When there is a mechanical stress applied to the piezoelectric material, it alters the structure, hence produces electricity. Reverse phenomenon occurred when there is an electricity applied, the piezoelectric material will change its shape. Under a mechanical stress, the ions in the crystal structure change its position from a balance positive and negative charge to a dipole moment. This causes the charge to be unbalanced and thus creating a potential energy or voltage across it [6]. The electrical charges can be collected at the piezoelectric surface using a simple electrode [7].

The typical structure of piezoelectric harvester is the cantilever type. The cantilever type used in this research are bimorph or double layer piezoelectric as shown in Figure 2.1.

Piezoelectric materials are attached to both sides of the strain or cantilever beam to optimize the vibration energy. This piezoelectric cantilever experienced a kinetic energy from surrounding vibration causing it to move upwards and downwards. When the beam is at the downward position, the upper piezoelectric material experienced a strain force thus producing electricity. Similar phenomenon occurred when the beam is at upward position [8]. This vibration energy harvester produces an AC output and which later to be rectified to a clean DC source [9].

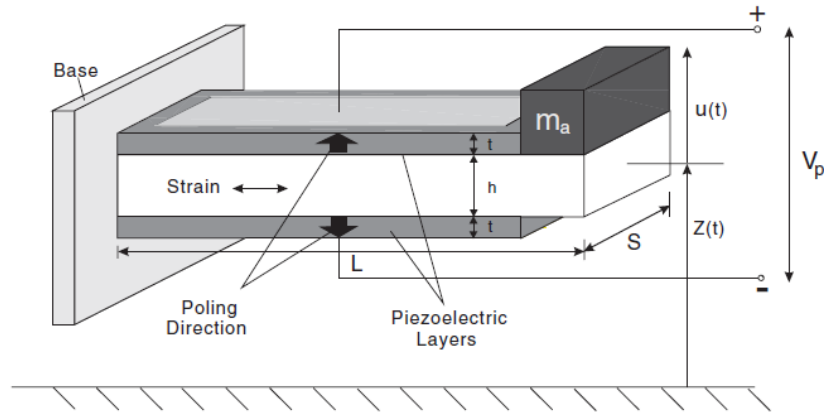


Figure 2.1: Piezoelectric Bimorph Cantilever Mechanism [10]

The conversion of mechanical energy to electrical energy can be analyzed with mass, spring and damper model as shown in Figure 2.2. Utilizing Newton's 2<sup>nd</sup> law of motion, the mechanical equation [11] can be derived as follows:

$$M\ddot{x} + B\dot{x} + Kx + Fe = -M\ddot{y} \quad (1)$$

Where,

M = Mass of load

B = Damping coefficient

K = Spring constant

Fe = Electrical force

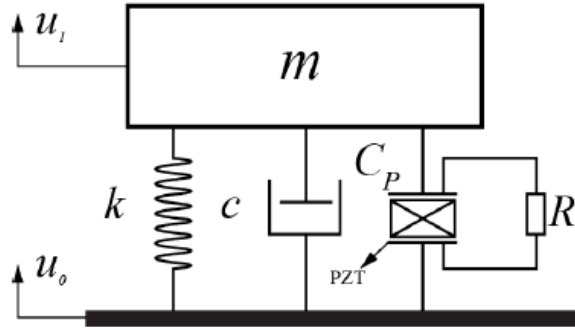


Figure 2.2: Mass, spring and damper model for Piezoelectric Energy Harvester [11].

### 2.3 Magnetostrictive Mechanism

The magnetostrictive term originated from Magnetostriction which is defined as expanding and shrinking of ferromagnetic material whenever a magnetic field is presence. Applying stronger magnetic field would increase the expanding and shrinking of the material. The magnetostrictive effect on the other hand is the reverse process of magnetostriction. Magnetostrictive effect or else known as Villari effect occurs when there is an external mechanical stress applied to the material, producing a change in magnetic flux, hence a magnetic field is produced. If a pick-up coil is wound around the magnetostrictive material, the change in magnetic flux density will induced the voltage in the pick-up coil. Similar phenomenon would occur if vibration energy from surrounding is applied to the material [12].

The magnetostrictive material is responsible to convert vibration energy into electrical energy. The most famous materials are Terfenol-D, TbDyFe and Galfenol, FeGa. Both are alloys that are normally used in energy harvesting research. Galfenol has a higher stiffness compared to Terfenol-D, making it more suitable for cantilever type or longitudinal stress-type energy harvesting [13]. Figure 2.3 illustrates the proposed model for magnetostrictive cantilever mechanism.



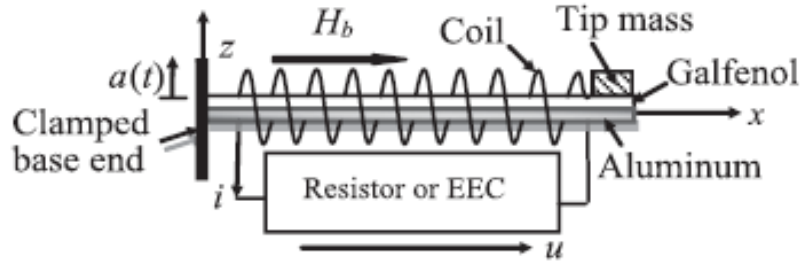


Figure 2.3: Magnetostrictive Cantilever Mechanism [13]

The conversion of mechanical energy to electrical energy for magnetostrictive can also be analyzed with mass, spring and damper model as shown in Figure 2.2. Based on Newton's 2nd law of motion, the mechanical equation [14] can be derived as follows:

$$M\ddot{x} + B\dot{x} + Kx + Fm = -M\ddot{y} \quad (2)$$

Where,

M = Mass of load

B = Damping coefficient

K = Spring constant

Fm = Magnetic force

## 2.4 Hybrid Energy Harvesting

In this research, both the piezoelectric and magnetostrictive energy harvesters are combined to form a hybrid energy harvester. Both piezoelectric and magnetostrictive harvesters captured and converted the vibration energy independently. This is necessary as both piezoelectric and magnetostrictive will capture different resonant frequencies. The output from both harvesters are fed into power management circuit. The output from both harvesters are in AC mode and need to be converted to DC power using a rectifier circuit. The converted power is then smoothed and regulated to produce a clean DC power. The clean DC power is then stored into energy storage such as battery or supercapacitor to

power up small powered device such as environmental sensor. Figure 2.4 demonstrate the proposed block diagram of energy harvesting module for this research.

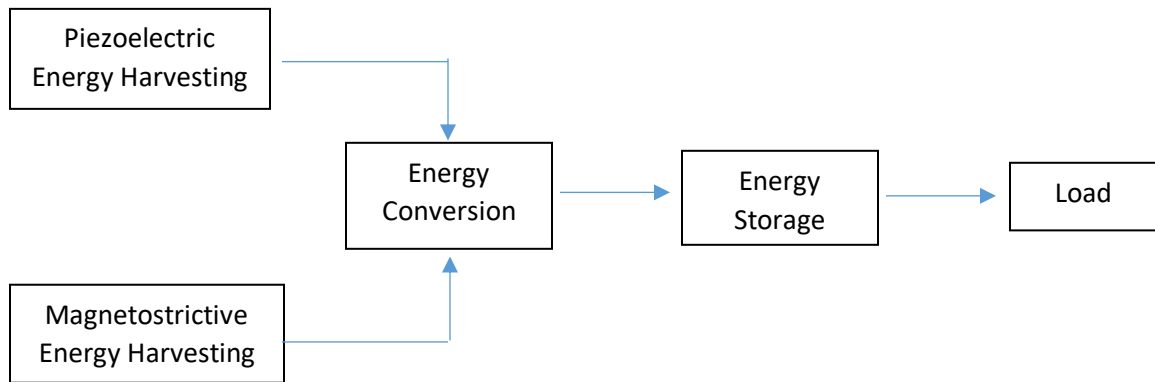
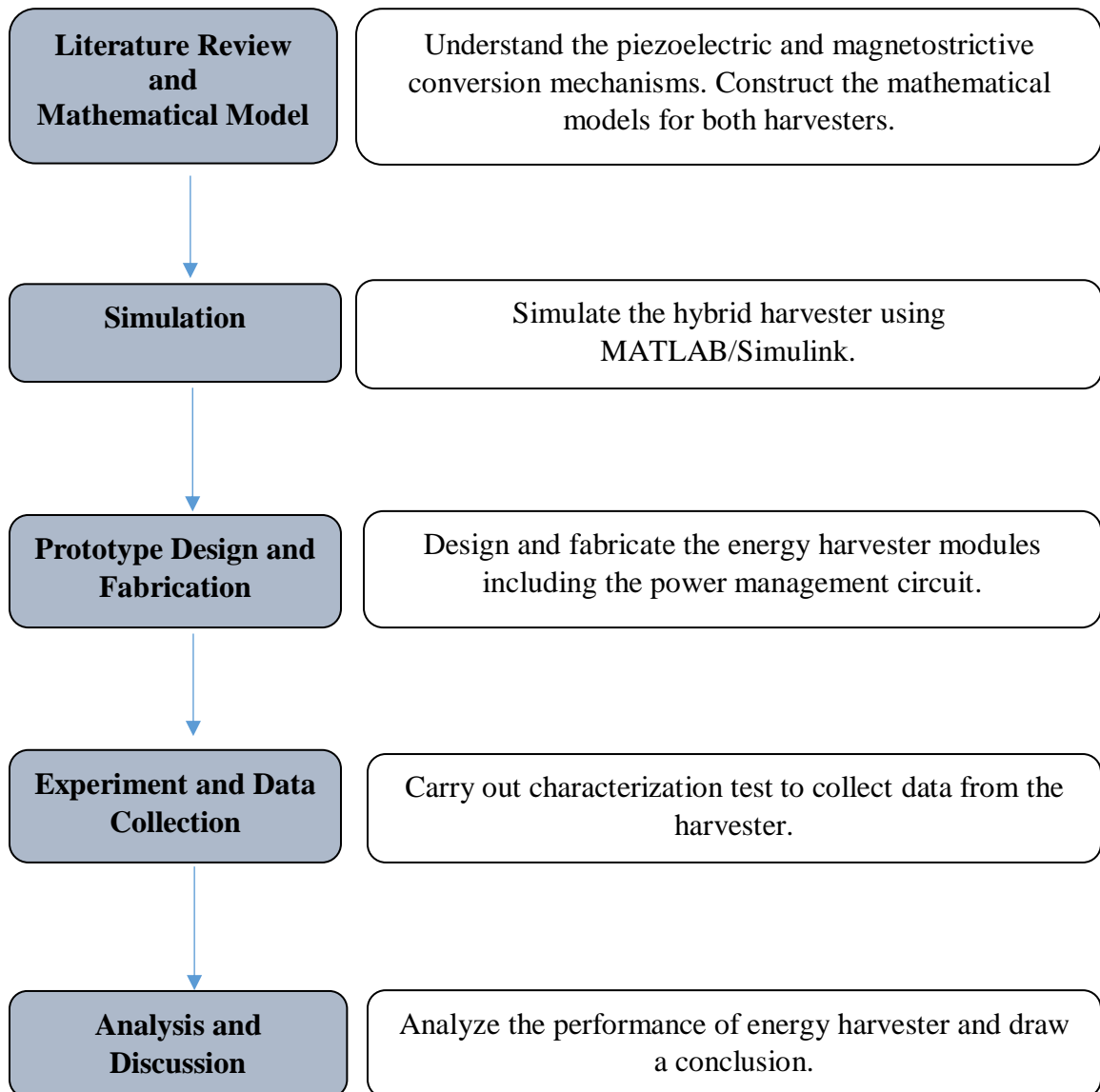


Figure 2.4: Block diagram representing the Energy Harvesting Module.

## CHAPTER 3

### METHODOLOGY

The methodology of this research can be represented as a process flowchart below.



### 3.1 Gantt chart

No	Detail Work	1	2	3	4	5	6	7	8	9	10	11	12	13	14
1	Title Selection	■													
2	Gather information from Research Papers	■	■	■	■	■									
3	Design Concept	■	■	■	■	■									
4	Extended Proposal						■								
5	Mathematical Model						■	■							
6	Simulation (Simulink)						■	■	■	■					
7	Proposal Defense									■					
8	Subsystem Design									■	■	■	■		
9	Initial Circuit Design													■	■
10	Material and Components Selection													■	■
11	Draft Interim Report													■	
12	Final Interim Report														■

Figure 3.1: Gantt chart for FYP 1

No	Detail Work	1	2	3	4	5	6	7	8	9	10	11	12	13	14	15
1	Research on Suitable Material	█	█													
2	Initial Prototype Design and Connection	█	█													
3	Material Selection and Purchase Order			█	█											
4	PCB design for Power Management Circuit					█	█	█								
5	Prototype Assembly							█	█							
6	Progress Report							█								
7	Experiment and Data Collection								█	█	█					
8	PRE-SEDEX									█						
9	Troubleshooting and Prototype Modification										█	█	█	█		
10	Draft Report													█		
11	Final Report and Technical Paper														█	
12	VIVA															█

Figure 3.2: Gantt chart for FYP 2

### 3.2 Project Milestone

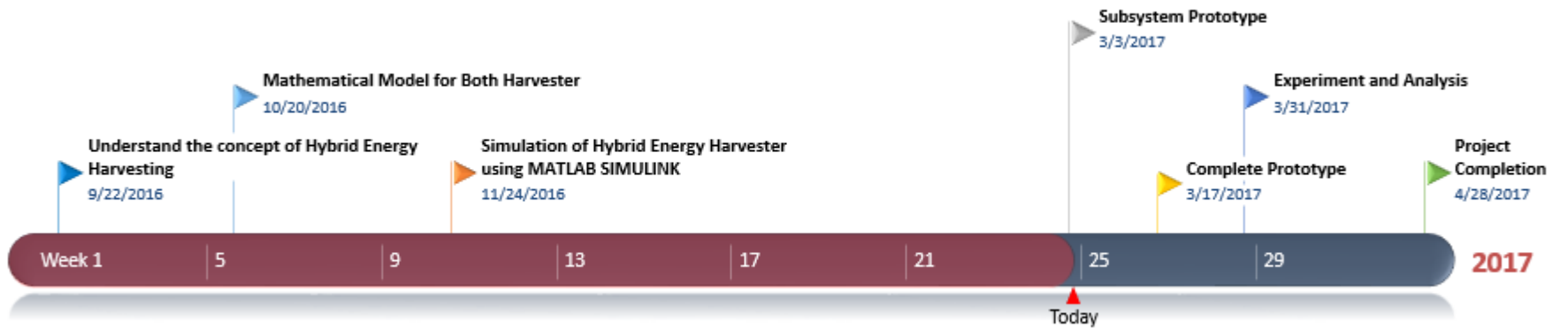


Figure 3.3: Project Milestone

### 3.3 Mathematical Model

#### 1) Equation for Piezoelectric

$$M\ddot{x} + B\dot{x} + Kx + Fe = -M\ddot{y} \quad (1)$$

where,

$\ddot{y} = a$  = acceleration of input vibration

Equation (1) describe the mechanical equation of the piezoelectric based on mass, damper and spring model. The electric force,  $Fe$  is the electrical energy that is converted from the mechanical energy.

The equation of the electric force is given by

$$Fe = \alpha Vp \quad (3)$$

where,

$\alpha$  = force factor

$Vp$  = Voltage across Piezoelectric

By rearranging the equation of current, we can yield the electrical equation for the piezoelectric

$$Vp = \frac{Vp}{CpR} + \frac{\alpha\dot{x}}{Cp} \quad (4)$$

Where,

$Cp$  = Blocking capacitance of piezoelectric

$R$  = Load resistance

Finally we can obtained a full equation of piezoelectric as follows

$$\ddot{x} = -\frac{B}{M}\dot{x} - \frac{K}{M}x - \frac{\alpha Vp}{M} - a \quad (5)$$

Equation (4) is then used to simulate the block diagram in MATLAB/Simulink.

## 2) Equation for Magnetostrictive

$$M\ddot{x} + B\dot{x} + Kx + Fm = -M\ddot{y} \quad (2)$$

where,

$\ddot{y} = a$  = acceleration of input vibration

Equation (5) describes the mechanical equation of the piezoelectric based on mass, damper and spring model. The magnetic force,  $Fm$  is the electrical energy that is induced from the mechanical energy applied on magnetostrictive.

The equation of the magnetic force is given by

$$Fm = GI \quad (6)$$

where,

$G$  = Gyrator ratio

$I$  = Induced current in coil

By rearranging the equation of current, we can yield the electrical equation for the piezoelectric

$$\dot{i} = \frac{G}{L}\dot{x} - \frac{IR}{L} \quad (7)$$

Where,

$L$  = Coil inductance

$R$  = Load resistance

Finally we can obtained a full equation of magnetostrictive as shown below

$$\ddot{x} = -\frac{B}{M}\dot{x} - \frac{K}{M}x - \frac{GI}{M} - a \quad (8)$$

Equation (8) is then used to simulate the block diagram in MATLAB/Simulink.



### 3.4 Simulink Block

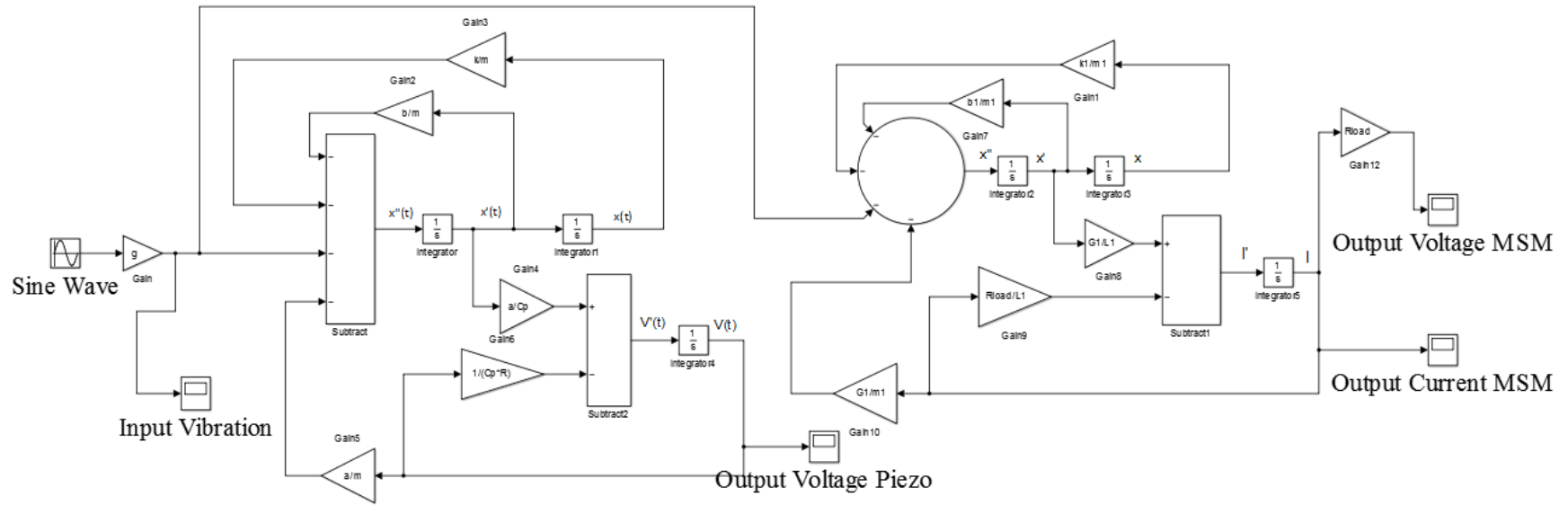


Figure 3.4: Simulink Block of the Hybrid Energy Harvester.

### 3.5 Table of Parameters

In order to simulate equation (5) and (8) with MATLAB/Simulink, several parameters value are needed. These values are leveraged from research papers based on similar energy harvesting project. The parameters are shown in table 3.1 and table 3.2. The initial frequency and vibration acceleration in this simulation is set at 100 Hz and  $9.81\text{ms}^{-2}$ .

Table 3.1: Simulation parameters for Piezoelectric [11]

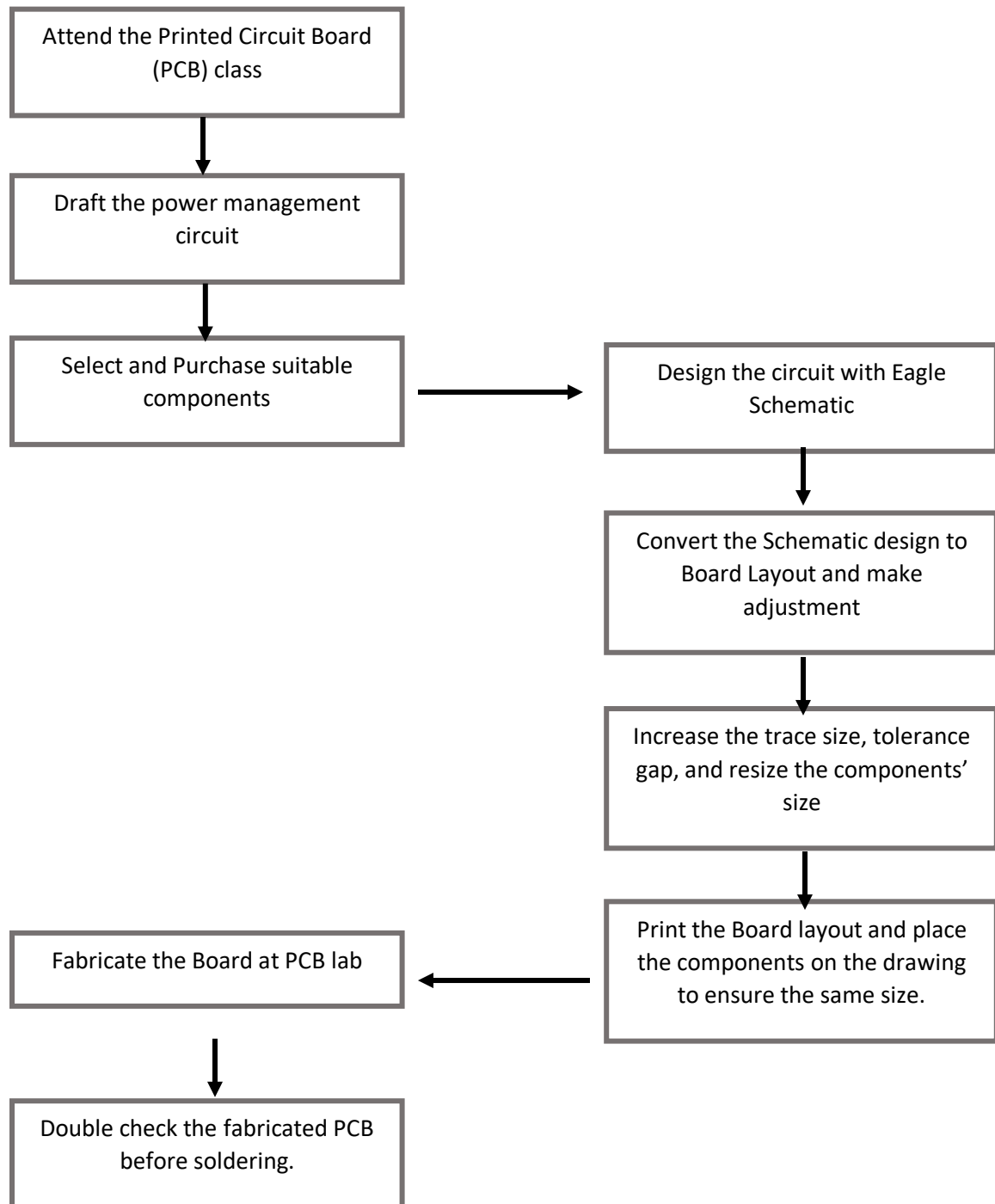
Parameter	Symbol	Value	Unit
Mass	M	$8.4 \times 10^{-3}$	kg
Damping Coefficient	B	0.154	N.s/m
Spring Constant	K	$2.5 \times 10^{-4}$	N/m
Blocking Capacitance	Cp	$1.89 \times 10^{-8}$	F
Force factor	$\alpha$	$1.52 \times 10^{-3}$	N/Volt
Load resistance	R	30669.6	Ohm

Table 3.2: Simulation parameters for Magnetostrictive [15]

Parameter	Symbol	Value	Unit
Mass	M	$1 \times 10^{-3}$	kg
Damping Coefficient	B	0.24	N.s/m
Spring Constant	K	$0.569 \times 10^{-3}$	N/m
Coil inductance	L	$47.16 \times 10^{-3}$	H
Gyrator ratio	G	0.1448	N/Ampere
Load resistance	R	180	Ohm

### 3.6 Designing Power Management Circuit

There are several steps taken in order to design the power management circuit on a Printed Circuit Board (PCB). The steps are shown in the flowchart below.



### 3.7 Components Selection for PCB design

Before designing the PCB, all the components have to be selected and purchased upfront to avoid any problems such as obsolete item. These components parts and values are taken referred from other research papers. All electrical components are shown in Table 3.3 below.

Table 3.3: Bill of Material for the PCB [16]

Component	Value	Vender	Manufacturing Part No.
L1	22 $\mu$ H	Sumida Co.	CDRH6D28NP-220NC
C1~C4	0.22 $\mu$ H	AVX Co.	12065C224KAT2A
C5	3F	NessCap Co.	ESHSR-0003C0-002R7
C6	47 $\mu$ F	AVX Co.	F930J476MAA
C7	10 $\mu$ F	AVX Co.	TPSD106K035R0125
D1~D6	N/A	Diodes Inc.	BAT54WS-7-F
R1	1 M $\Omega$	Panasonic - ECG	ERJ-P06J105V
R2	330 k $\Omega$ ~3 M $\Omega$	Panasonic - ECG	EVM-7JSX30BY5
R3	220 k $\Omega$	Panasonic - ECG	ERJ-6GEYJ224V

### 3.8 Power Management Circuit

#### 3.8.1 Schematic Design

The schematic design for the power management circuit is shown in Figure 3.5 below. This circuit consist of rectifying circuit, DC-DC Boost Converter, Supercapacitor and Smart Regulator IC MAX 1795. Several pinheads are placed for troubleshooting purposes at every section of the circuit.

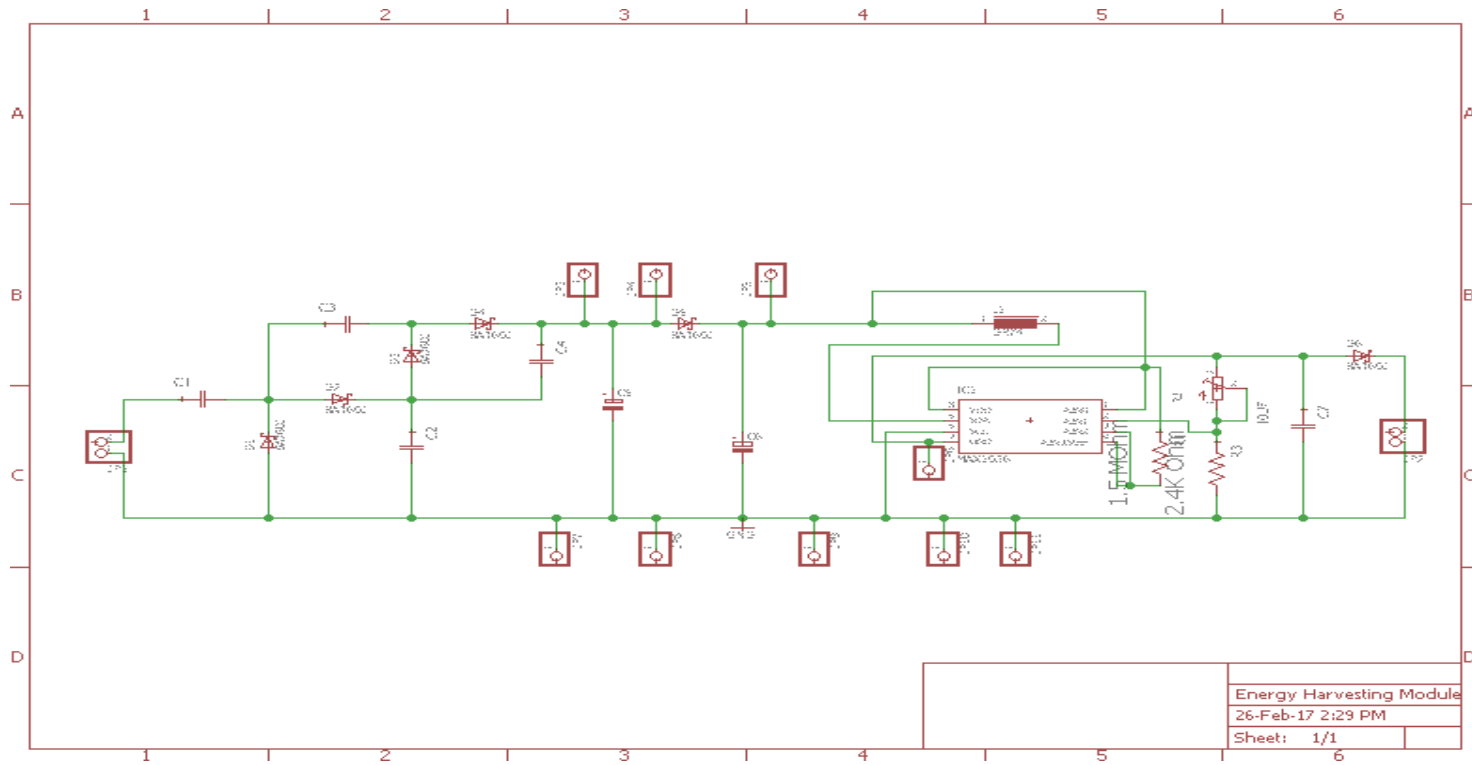


Figure 3.5: Schematic for Power Management Circuit [16]

### 3.8.2 Board Layout

The Schematic design is then converted to layout. In this board layout, we have to arrange all the components closely to each other and accordingly with the minimum tolerance. The position of the components are based on the functions. Figure 3.6 below shows the 100% completed board connection after auto routing.

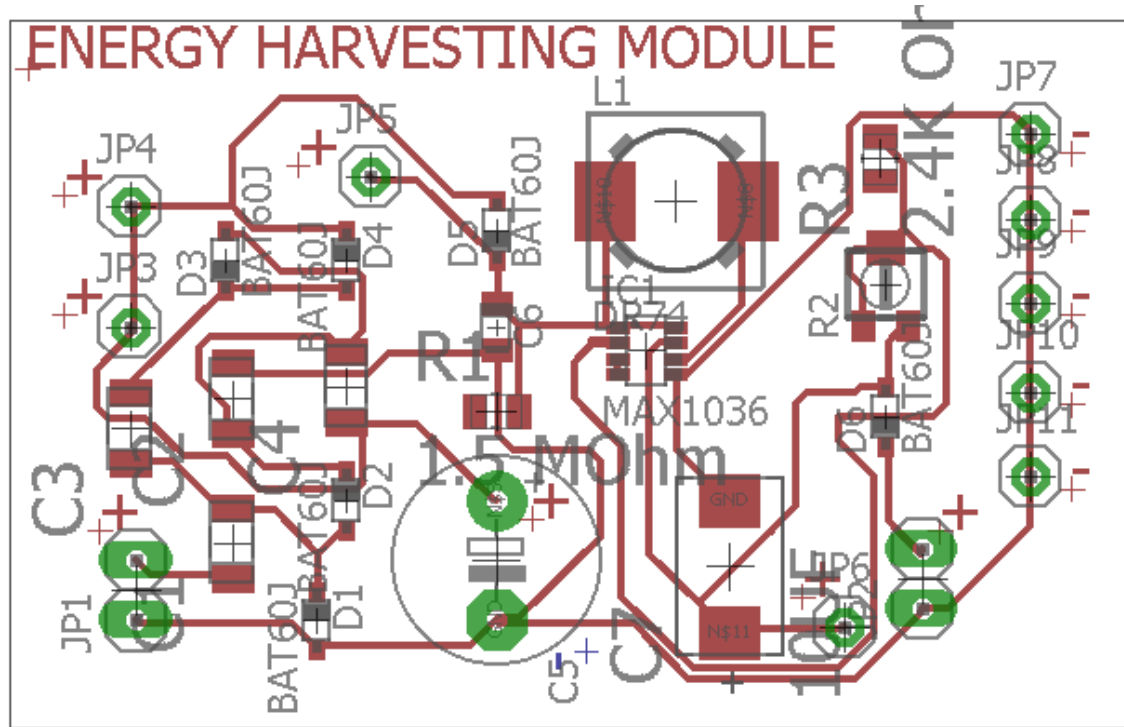


Figure 3.6: Equivalent Board for Power Management Circuit

### 3.8.3 Board Adjustment

Figure 3.7 shows the final modification of the board layout before fabrication process. In this area, we can resize the components' size if there is no library provided. Datasheet for every component is needed for the resizing purpose. Once everything is adjusted, it is ready for fabrication.

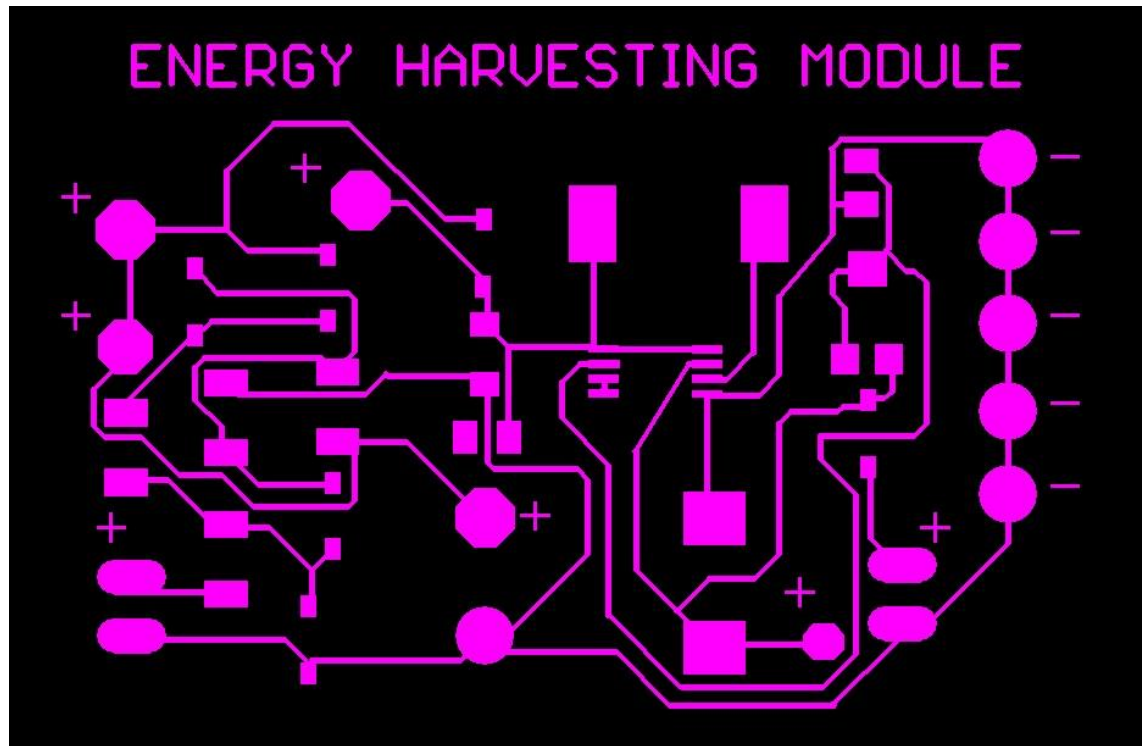


Figure 3.7: Modified Board

### 3.8.4 Fabricated PCB

Finally the board is successfully fabricated as shown in Figure 3.8. The size of the PCB board is compared with a 20 cent coin. All the selected components are soldered on the PCB board.

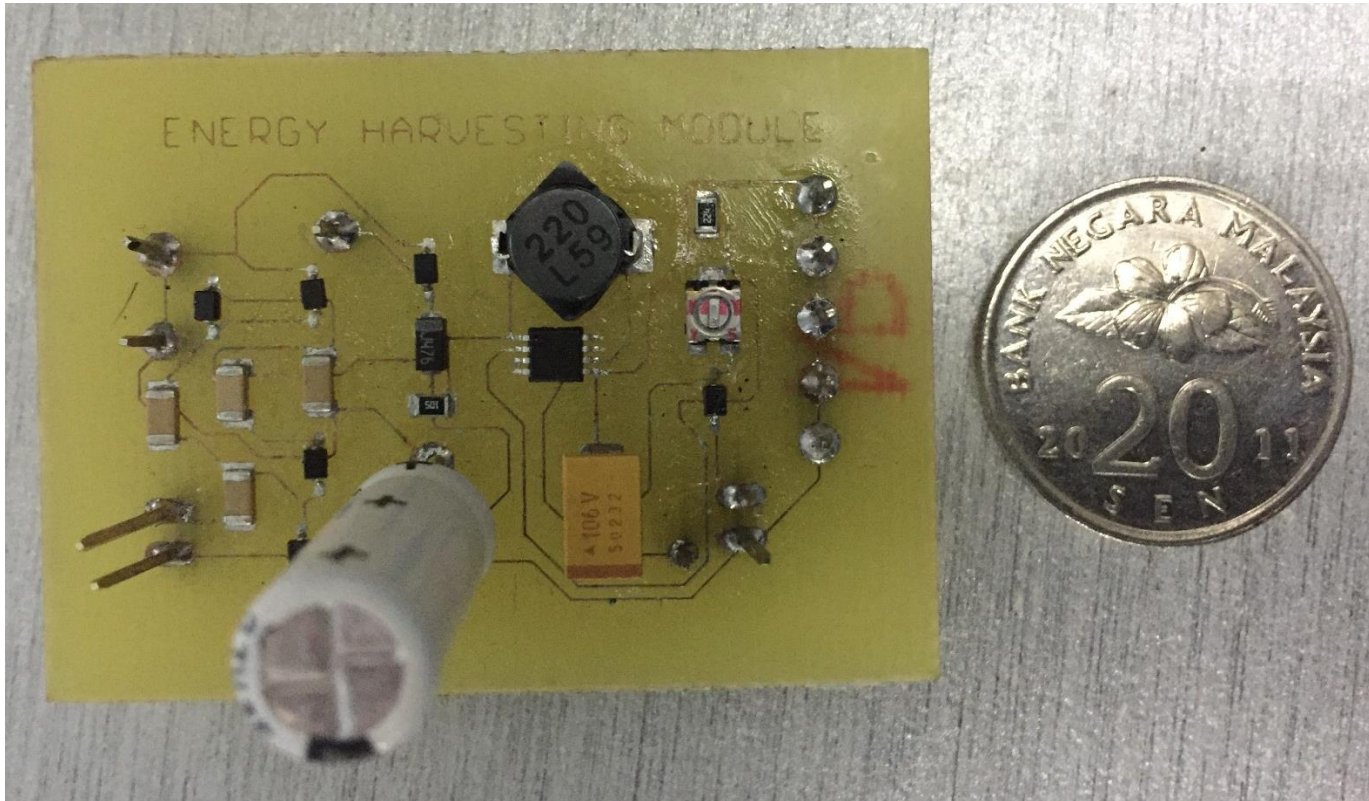


Figure 3.8: Completed PCB Board



### 3.9 Prototype Design Piezoelectric Energy Harvester

Piezoelectric energy harvester is designed using TinkerCad online software. Round shape is used as the base of the harvester to provide great stability and matching the vibration shaker base. The designed harvester is shown in Figure 3.9 and 3.10 below.

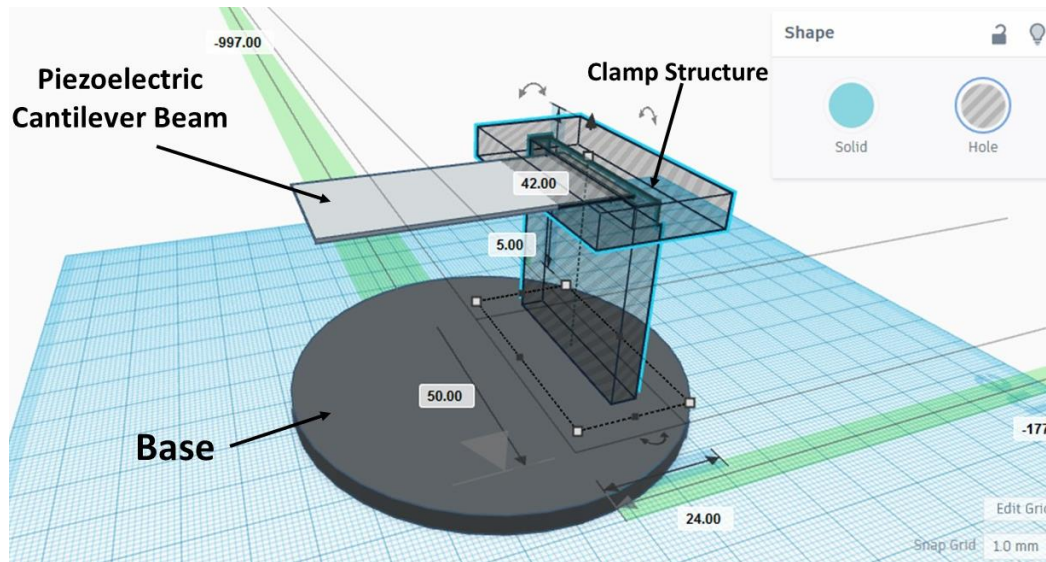


Figure 3.9: Side View

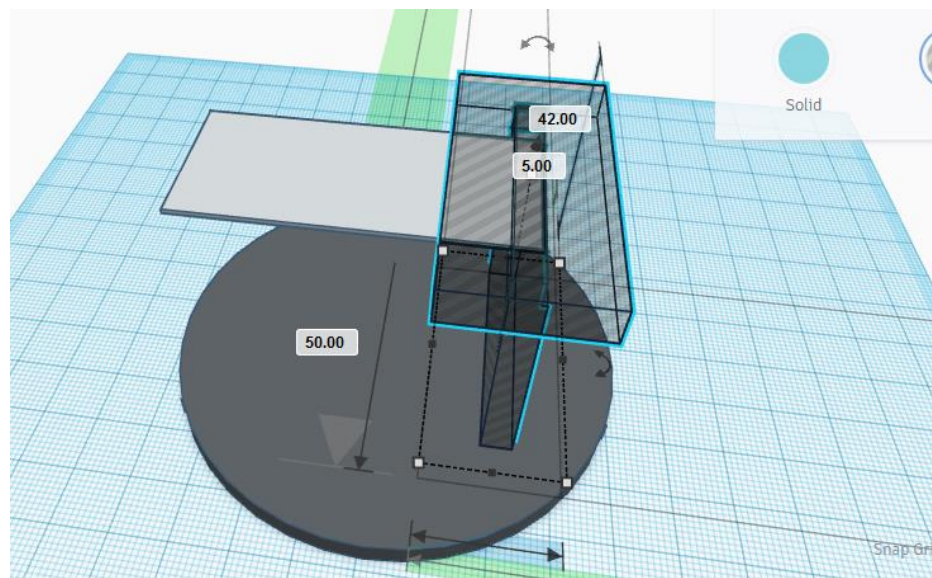


Figure 3.10: Top Side View

### 3.10 Prototype Design of Electromagnetic Energy Harvester

Due to unavailability of the Magnetostrictive material, the Electromagnetic energy harvester is developed as a substitute due to the fact that both methods are using electromagnetic conversion or Faraday's Law. Since both methods are using pick-up coil, the change of magnetic flux in the copper coil will induce a voltage in the coil itself and if the coil is connected in a closed circuit, the current will flow. The only difference between these two methods is, the Magnetostrictive consist of ferromagnetic materials that produce magnetic field when mechanical force is applied to it. In order to substitute it with Electromagnetic, author uses a Neodymium magnet (NdFeB) which is a type of rare-earth magnet to produce the magnetic flux required.

Similar to the Piezoelectric, Electromagnetic energy harvester is designed using TinkerCad online software. Most of the design are similar except there are additional holder for copper coil beneath the cantilever beam. The size of the cantilever beam is also relatively small compared to the Piezoelectric. Figure 3.11 and 3.12 illustrate the design from two point of view. Figure 3.13 shows the integration of both harvesters into a single device.

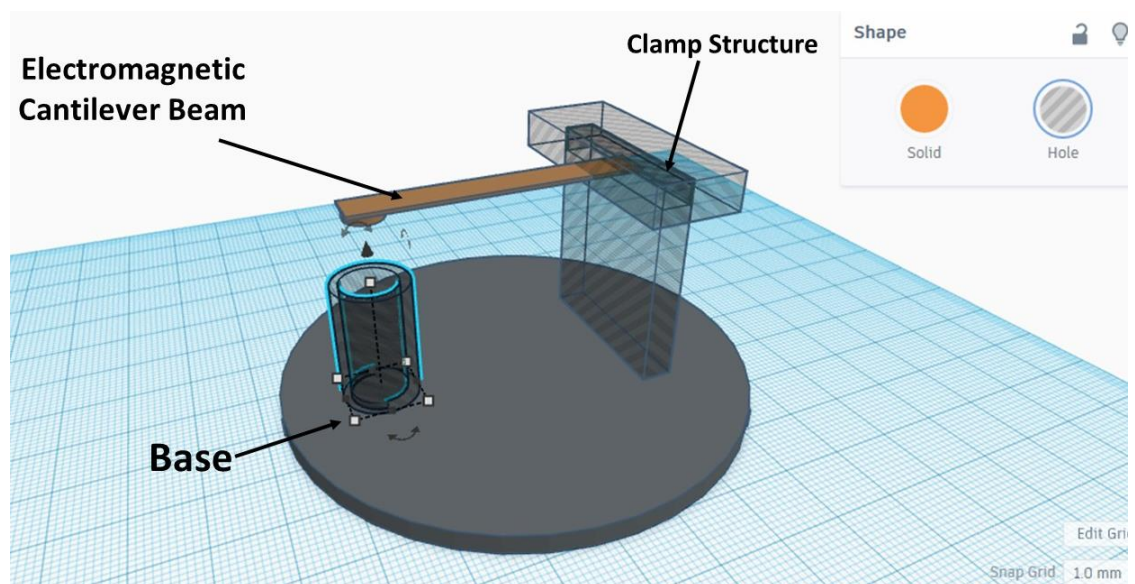


Figure 3.11: Side View

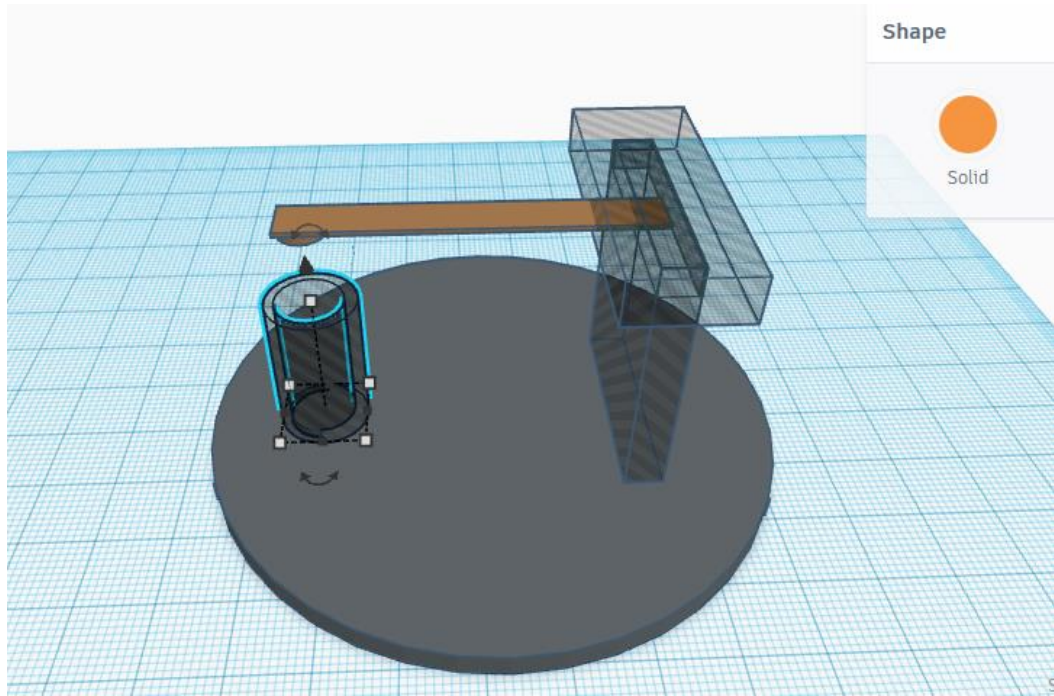


Figure 3.12: Top Side View

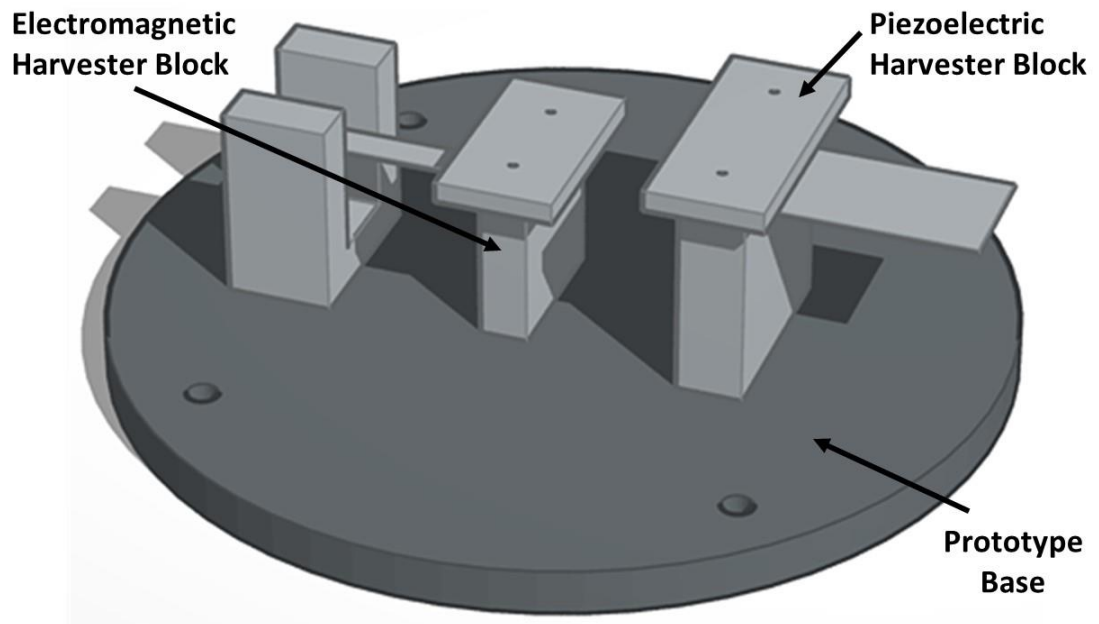


Figure 3.13: Hybrid Energy Harvester Prototype which consist of Piezoelectric and Electromagnetic Harvester.



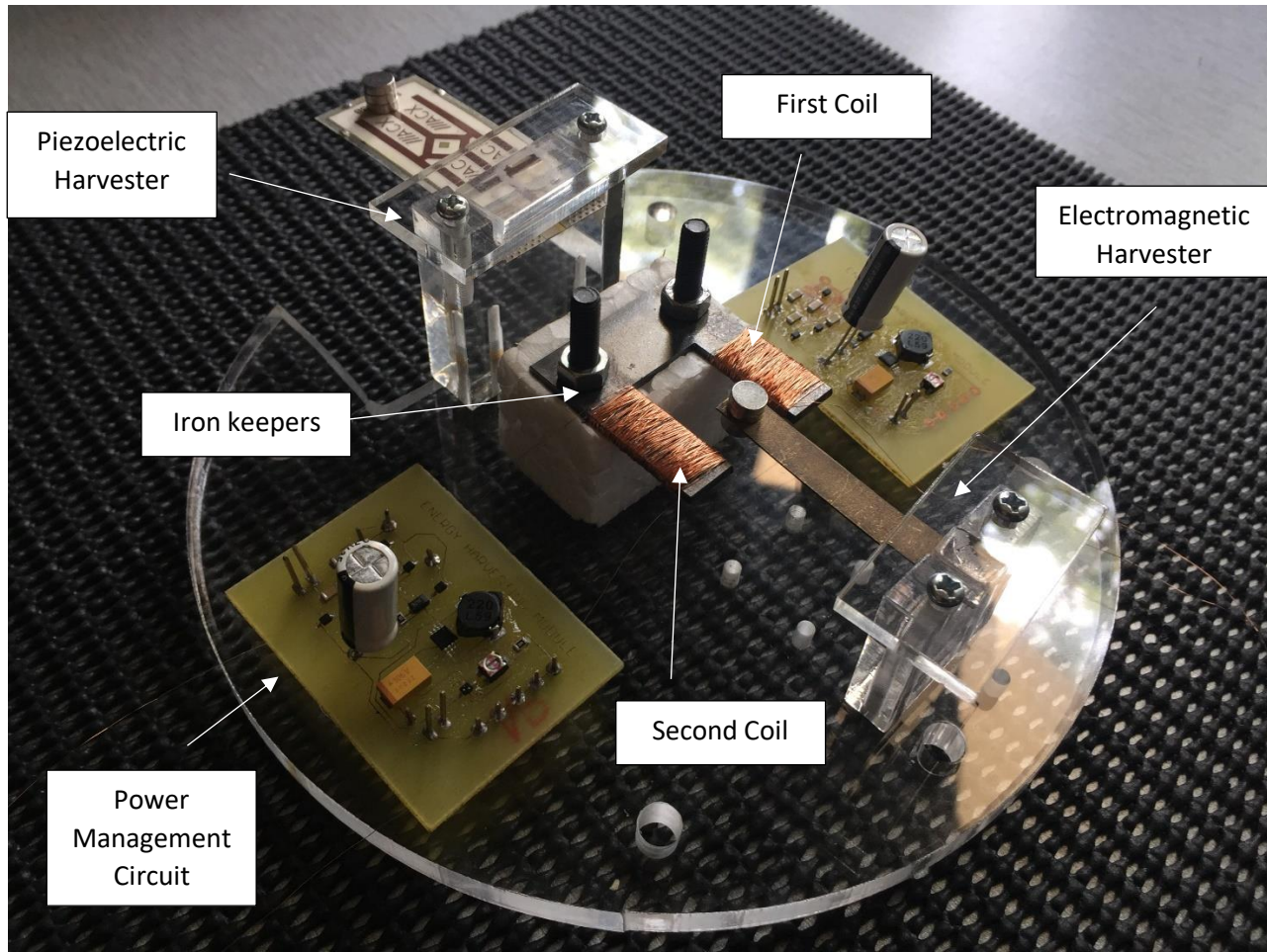


Figure 3.14: Completed Hybrid Energy Harvester

## CHAPTER 4

### RESULTS AND DISCUSSION

#### 4.1 Output Voltage of Piezoelectric

The output voltage obtained from the piezoelectric block is shown in Figure 4.2 based on the simulation done with MATLAB/Simulink. The output voltage obtained is sinusoidal shape as the input vibration in figure 4.1 is a sinusoidal wave. This shows that the system is linear. Moreover, the  $180^\circ$  phase difference between the input vibration and the output voltage proves that the energy harvester block diagram is properly constructed.

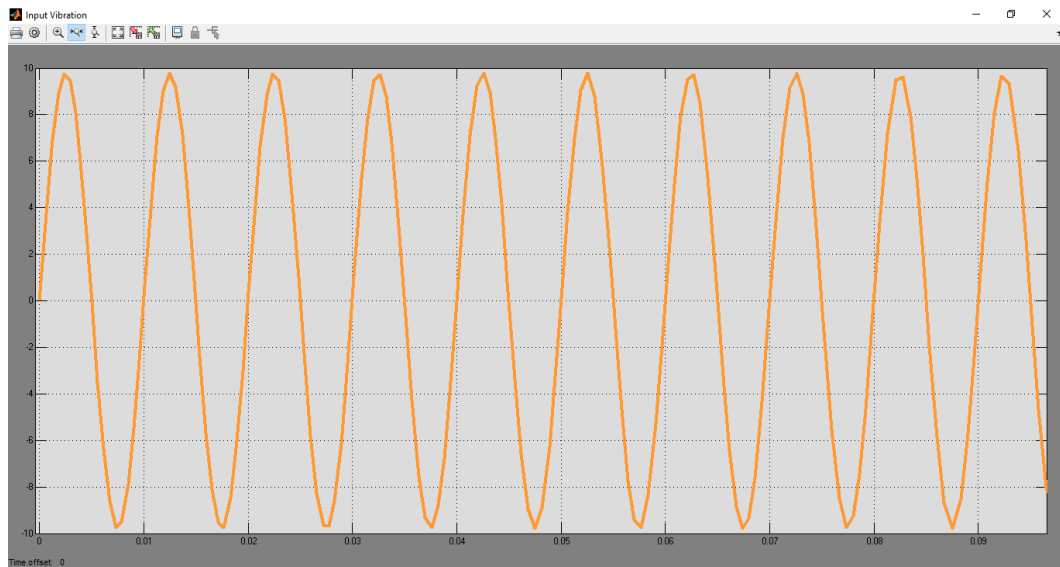


Figure 4.1: Input vibration that is applied to Piezoelectric

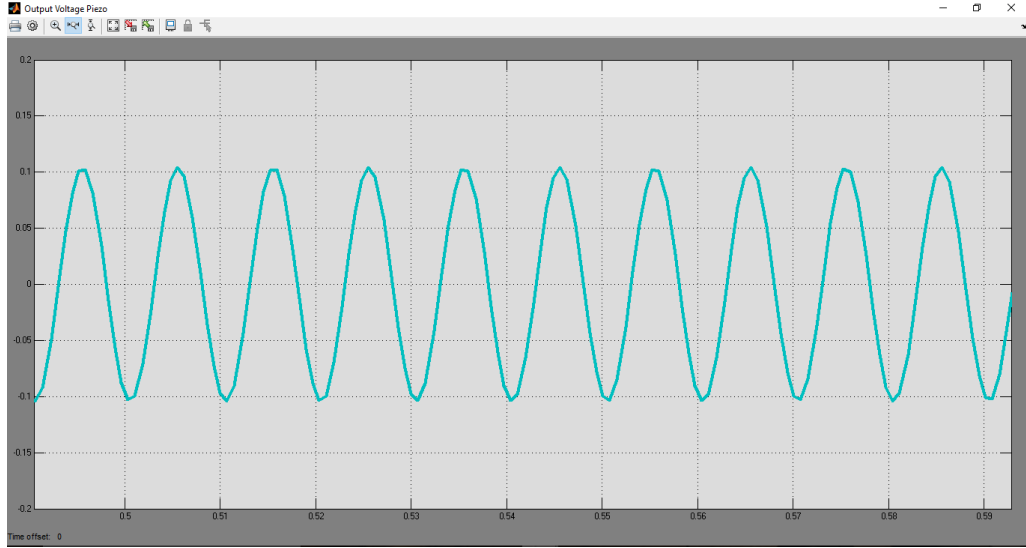


Figure 4.2: Output voltage of Piezoelectric

In order to find the resonance frequency of the piezoelectric, a graph of voltage vs frequency is plotted as shown in figure 4.3. Different frequency range is used to observe the output voltage produced. It can be seen in figure 4.3 that the peak voltage of 1.02 V occurs at 300Hz. Thus, it can be deduced that piezoelectric resonates at 300Hz. Another part that should be examined is when the value of frequency is increased from the resonance frequency, the voltage produced by the piezoelectric is now become negligible and approaching zero. At these frequencies, the piezoelectric become unstable.

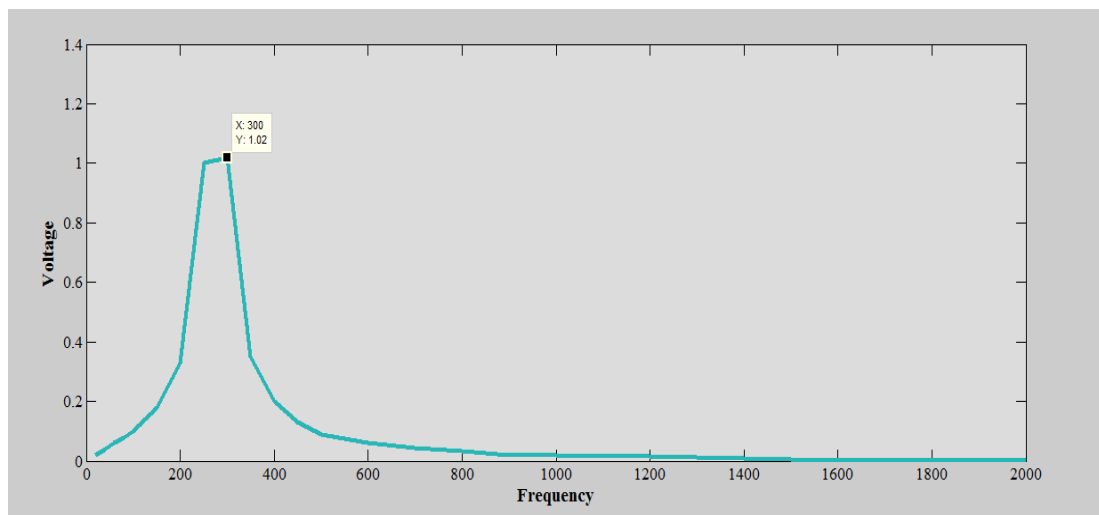


Figure 4.3: Voltage vs frequency in Piezoelectric

## 4.2 Output Voltage of Magnetostrictive

The output voltage of the magnetostrictive block is shown in Figure 4.5 based on the simulation done with MATLAB/Simulink. The output voltage produced is sinusoidal shape as the input vibration in figure 4.4 is a sinusoidal wave. This indicates that the system is linear. Moreover, the  $180^\circ$  phase difference between the input vibration and the output voltage shows that the energy harvester block diagram is properly constructed.

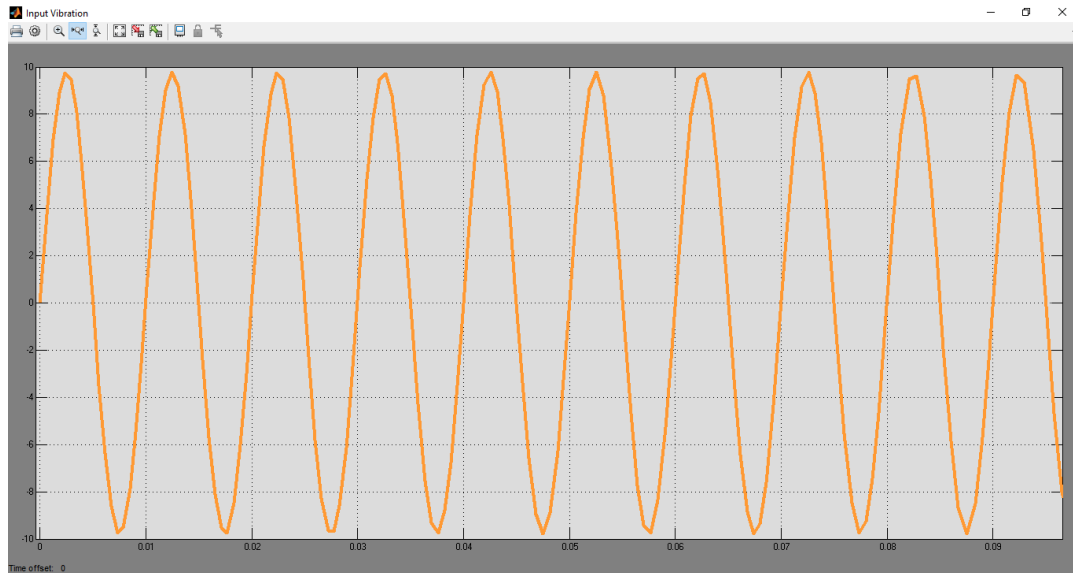


Figure 4.4: Input vibration that is applied to Magnetostrictive

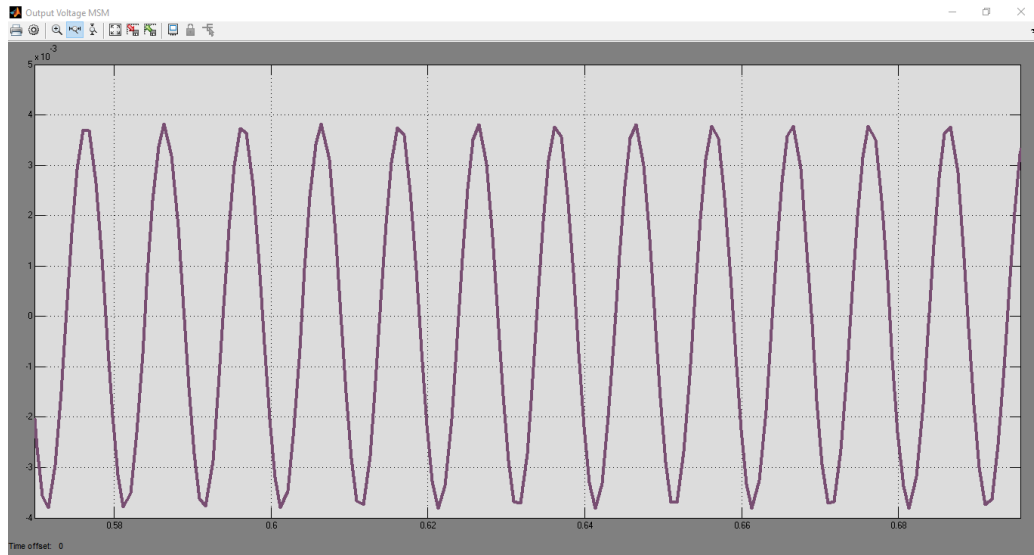


Figure 4.5: Output voltage of Magnetostrictive

A graph of voltage vs frequency is plotted as shown in Figure 4.6. Various frequency range is used to observe the output voltage produced. It can be seen in Figure 4.6 that the peak voltage produced at 100Hz is 3.47mV. Thus, it indicates that the magnetostrictive resonates at 100Hz. Another aspect that should be examined is when the value of frequency is increased from the resonance frequency, the voltage produced by the magnetostrictive becomes negligible and approaching zero. However this magnetostrictive harvester is quite stable at high frequency. The changes in the output voltage at high frequency is not that significant as compared to piezoelectric.

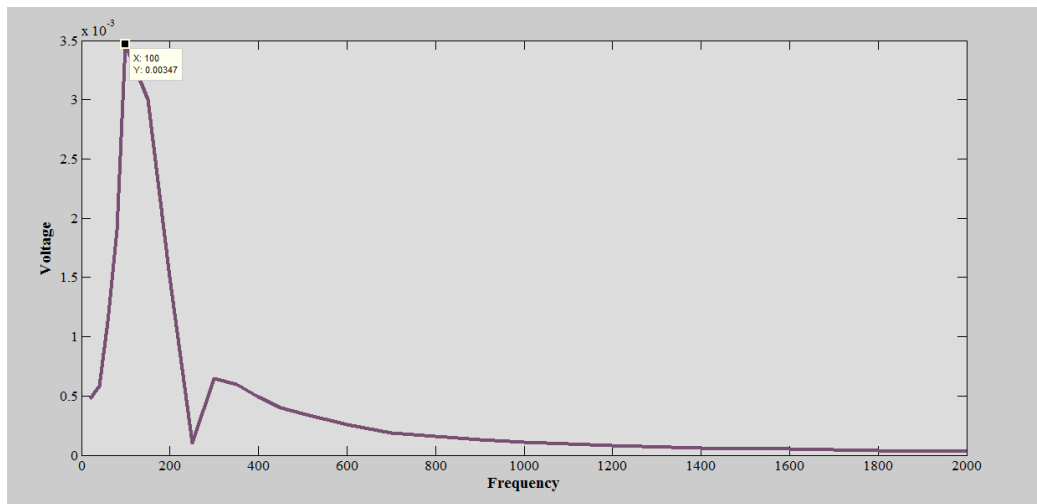


Figure 4.6: Voltage vs frequency in Magnetostrictive



### 4.3 Experimenting on Hybrid Energy Harvester

An experiment was conducted on the Hybrid Energy Harvester in order to identify the actual resonance frequency for each harvester. The equipment was set up as in Figure 4.7 and 4.8. In order to analyze the resonance frequency and the voltage produced, Dewesoft Software is used together with Digital Signal Analyzer.

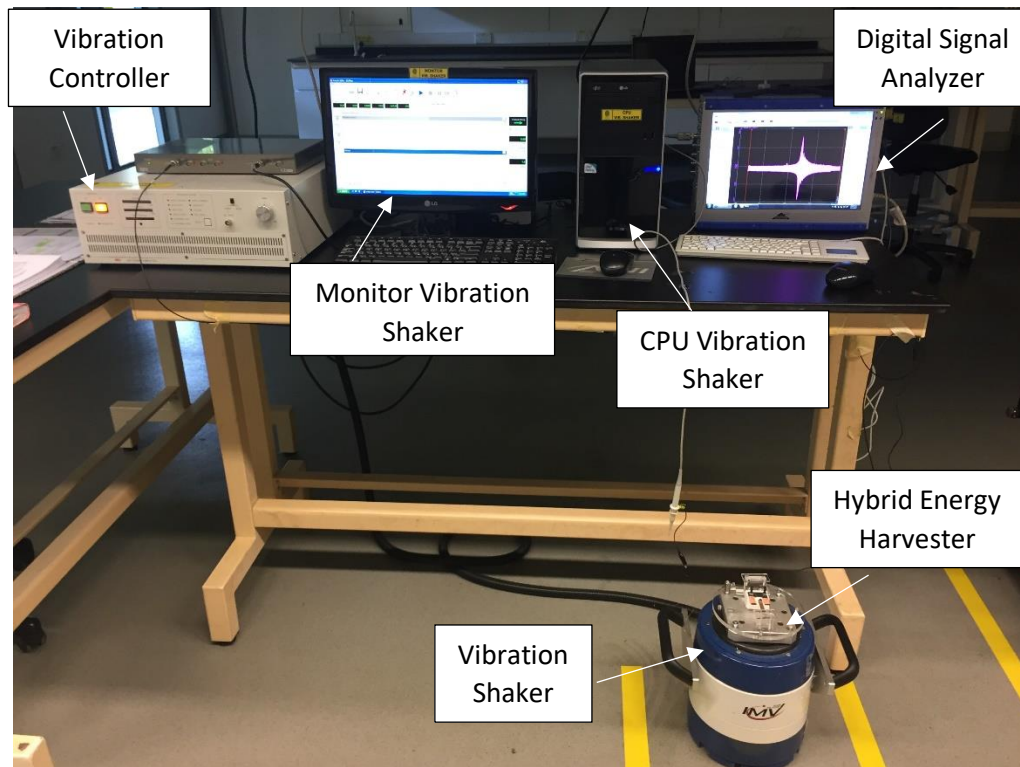


Figure 4.7: Equipment setup in the vibration lab.



Figure 4.8: Hybrid Energy Harvester on Vibration Shaker

Before experiment is conducted, several parameters are established in order to achieve the desired outcome. Table 4.1 and 4.2 shows the components on each piezoelectric and electromagnetic energy harvester. The characteristic for each components are set to specific conditions in order to observe the output from both harvesters. The frequency range and vibration acceleration in this experiment is set between 0 - 100 Hz and  $9.81\text{ms}^{-2}$ .

Table 4.1: Experiment parameters for Piezoelectric

<b>Component</b>	<b>Characteristic</b>			
	<b>Material</b>	<b>Dimension</b>	<b>Weight</b>	<b>Quantity</b>
<b>Piezoelectric</b>	Plumbum, Zirconate, Titanate (PZT)	55.3mm x 23.3mm x 0.46mm	2.8g	1 piece
<b>Tip Mass</b>	Neodymium Iron Boron (NdFeB)	6 mm x 2mm Disc shape	0.8 gram each	6 pieces

Table 4.2: Experiment parameters for Electromagnetic

<b>Components</b>	<b>Characteristic</b>			
	<b>Material</b>	<b>Dimension (mm)</b>	<b>Weight (g)</b>	<b>Quantity (pieces)</b>
<b>Magnet</b>	Neodymium Iron Boron (NdFeB)	6 mm x 2mm Disc shape	0.8 gram each	4 pieces
<b>Cantilever Beam</b>	Beryllium Copper (BeCu)	50mm x 7mm x 0.5mm	N/A	1 piece
<b>Pickup coil</b>	Enamelled Copper Wire	0.1 mm x 35m	N/A	2 pieces ( 200 turns each)

### 4.3.1 Resonance Frequency of Electromagnetic Energy Harvester

In this experiment, two coils are used to observe the resonance frequency. Figure 4.9 represents the voltage vs frequency graph of coil 1. A frequency range of 0-100Hz is used to observe the output voltage produced. It can be seen in Figure 4.9 that the peak voltage produced at 63.48Hz is 13.9mV. Thus, it indicates that this electromagnetic harvester resonates at 63.8Hz. However, different results are achieved in coil 2 as shown in Figure 4.10. Although it resonates at the same frequency as coil 1, there is a huge difference in output voltage produced. Coil 2 produced 3.57mV at resonance frequency. This occurred due to the density and the distance of coil winding from the magnet itself. Coil 1 has a denser coil winding and shorter distance compared to coil 2.

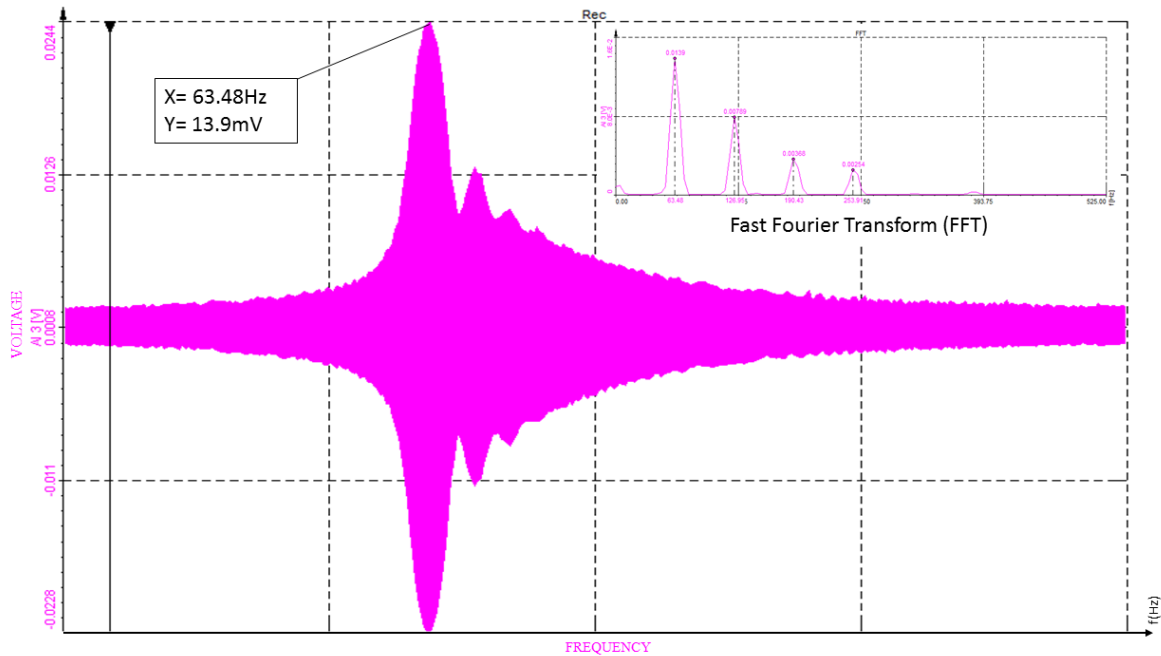


Figure 4.9: Voltage vs frequency in Coil 1

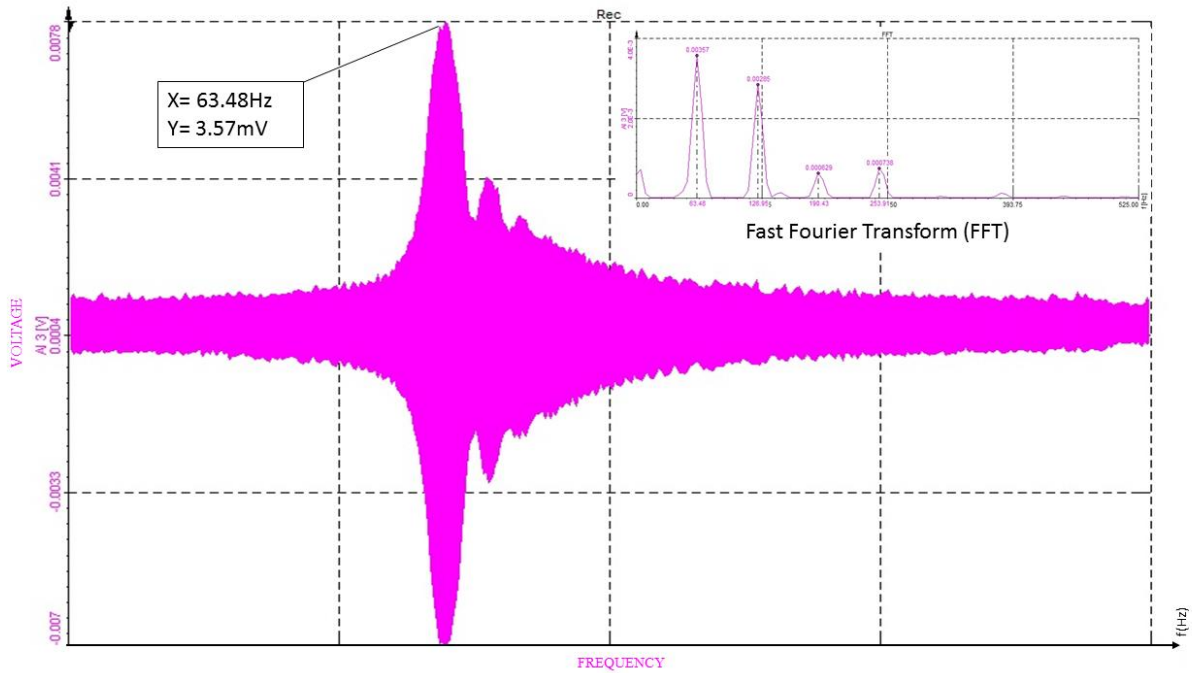


Figure 4.10: Voltage vs frequency in Coil 2

In order to maximize the output voltage of electromagnetic harvester, both coil 1 and coil 2 are connected in series. Theoretically the amount of voltage from both coil will add up and increase the output voltage of this harvester at resonance frequency. However based on figure 4.11, the output voltage produced is smaller, which is 2.9mV at 63.48Hz resonance frequency. There is an unknown lag between the two coils causing destructive interference to take place. The destructive interference between the two coils causes the voltage from both coils to cancel each other out, leaving only small fraction of voltage left. Thus only one coil is needed to produce the desired output.

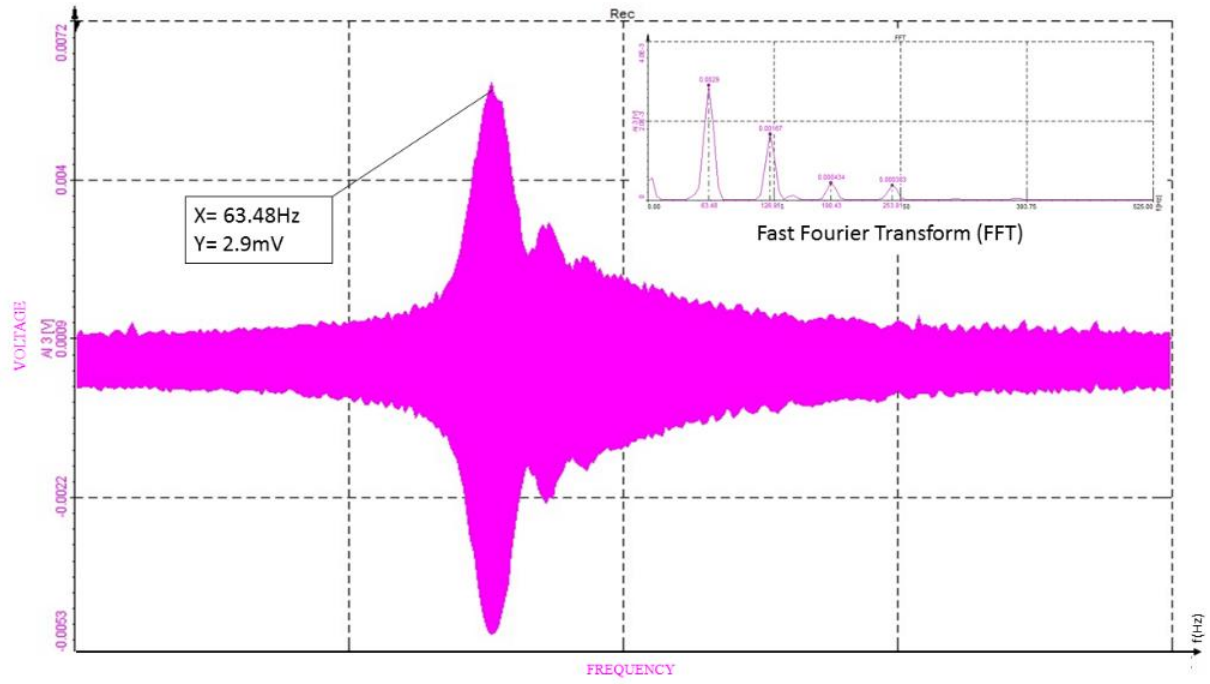


Figure 4.11: Voltage vs frequency in when Coil 1 and Coil 2 are connected in series.

### 4.3.2 Resonance Frequency of Piezoelectric Energy Harvester

In this experiment, six pieces of Neodymium Iron Boron (NdFeB) with total weight of 4.8 g is used as a tip mass for the piezoelectric cantilever. The purpose of the mass is to ensure that the piezoelectric harvester resonates at lower frequency than electromagnetic harvester. However the output voltage produced is much greater than the electromagnetic harvester. It can be seen in figure 4.12 that the peak voltage produced at 58.59Hz is 6.23V which exceeds the maximum voltage displayed by the software. The reason behind this is because the piezoelectric used in this experiment is highly fabricated by the industry compared to the electromagnetic harvester which is hand made. In order to integrate these two harvesters, more optimization are needed towards electromagnetic harvester due to its smaller output voltage. The electromagnetic harvester will become idle if the integration of both harvesters take place in this current condition.

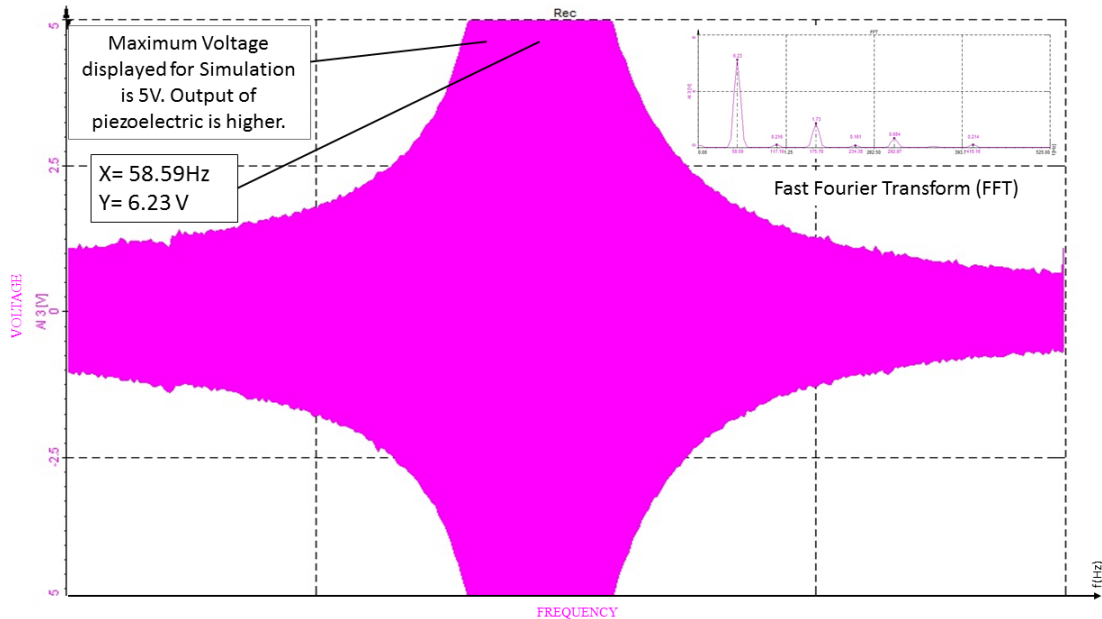


Figure 4.12: Voltage vs frequency in Piezoelectric

## **CHAPTER 5**

### **CONCLUSION AND RECOMMENDATION**

#### **5.1 Conclusion**

In conclusion, Hybrid Energy Harvester is a potential future renewable energy device. The ambient energy surrounding us has unlimited supply and by using this harvester we are able to benefit more from it. Moreover, we can reduce our dependency on fuel energy such as fossil fuel, natural gas and coal. The concept of hybrid energy harvesting is more efficient than the conventional energy harvester as it covers other bandwidth of frequencies making it feasible to power up low-powered devices. However more optimization is needed towards this hybrid harvester due to the large difference in output voltage from piezoelectric and electromagnetic energy harvester. More time and research are required which are not available in FYP level. The design of the hybrid energy harvester should be more specific to increase the efficiency of the harvester. As example, the gap between the iron keepers must be close enough to collect all the magnetic flux from the magnet. The objectives in this research have been achieved as the mathematical model for this hybrid energy harvester is successfully developed and simulated with MATLAB/Simulink. Moreover, the resonant frequency for each converting mechanism has been identified, which is important in deciding the suitable location to place the hybrid energy harvester later.

## **5.2 Recommendation**

1. Improve the design of the hybrid energy harvester to maximize the conversion of vibration energy.
2. More optimization towards electromagnetic energy harvester in order to produce sufficient power.
3. Use a power switching circuit that can efficiently switch power source whenever the vibration frequencies varies without leaving the load unsupplied.



## REFERENCES

- [1] M. R. B. Ahmad and M. H. B. M. Khir, "Design, analysis and fabrication of Electret-based micro-electromechanical systems energy harvester," in *National Postgraduate Conference (NPC), 2011*, 2011, pp. 1-4.
- [2] N. M. Ali, A. A. Mustapha, and K. S. Leong, "Investigation of hybrid energy harvesting circuits using piezoelectric and electromagnetic mechanisms," in *Research and Development (SCOReD), 2013 IEEE Student Conference on*, 2013, pp. 564-568.
- [3] R. Ambrosio, R. TorreAlba, J. F. Guerrero-C, V. Gonz, lez, A. Limon, *et al.*, "Energy harvesting combining three different sources for low power applications," in *Electrical Engineering, Computing Science and Automatic Control (CCE), 2015 12th International Conference on*, 2015, pp. 1-6.
- [4] B. Edwards, K. C. Aw, A. P. Hu, and L. Tang, "Hybrid electromagnetic-piezoelectric transduction for a frequency up-converted energy harvester," in *2015 IEEE International Conference on Advanced Intelligent Mechatronics (AIM)*, 2015, pp. 1149-1154.
- [5] T. Hehn and Y. Manoli, "Piezoelectricity and Energy Harvester Modelling," in *CMOS Circuits for Piezoelectric Energy Harvesters*, ed: Springer, 2015, pp. 21-40.
- [6] P. Dineva, D. Gross, R. Müller, and T. Rangelov, "Dynamic fracture of piezoelectric materials."
- [7] A. Telba and W. G. Ali, "Modeling and simulation of piezoelectric energy harvesting," in *Proceedings of the World Congress on Engineering*, 2012, pp. 4-6.
- [8] L. Zhang, "Analytical modeling and design optimization of piezoelectric bimorph energy harvester," The University of Alabama TUSCALOOSA, 2010.
- [9] P. Muralt, M. Marzencki, B. Belgacem, F. Calame, and S. Basrour, "Vibration energy harvesting with PZT micro device," *Procedia Chemistry*, vol. 1, pp. 1191-1194, 2009.


- [10] Y. Shu and I. Lien, "Analysis of power output for piezoelectric energy harvesting systems," *Smart materials and structures*, vol. 15, p. 1499, 2006.
- [11] H. Xiao, "A study of linear piezoelectric vibration energy harvesting technique and its optimisation," RMIT University, 2015.
- [12] A.-G. Olabi and A. Grunwald, "Design and application of magnetostrictive materials," *Materials & Design*, vol. 29, pp. 469-483, 2008.
- [13] S. Cao, S. Yang, J. Zheng, L. Zhang, and B. Wang, "An Equivalent Circuit Model and Energy Extraction Technique of a Magnetostrictive Energy Harvester," *IEEE Transactions on Applied Superconductivity*, vol. 26, pp. 1-6, 2016.
- [14] M. Oscarsson, "Modelling and design approaches of magnetostrictive actuators," 2007.
- [15] S. Naik, A. Phipps, V. In, P. Cavaroc, A. Matus-Vargas, A. Palacios, *et al.*, "Energy harvesting with coupled magnetostrictive resonators," in *SPIE Smart Structures and Materials+ Nondestructive Evaluation and Health Monitoring*, 2014, pp. 90570W-90570W-11.
- [16] L. Wang and F. Yuan, "Vibration energy harvesting by magnetostrictive material," *Smart Materials and Structures*, vol. 17, p. 045009, 2008.

# APPENDICES

## Appendix

- A Input Vibration settings for Simulink
- B Coding for Piezoelectric and Magnetostrictive Values
- C Coding for Resonance Frequency Graph
- D Datasheet for Piezoelectric

### Appendix A: Input Vibration settings for Simulink

 Source Block Parameters: Sine Wave1

Number of offset samples =  $\text{Phase} * \text{Samples per period} / (2 * \pi)$

Use the sample-based sine type if numerical problems due to running for large times (e.g. overflow in absolute time) occur.

Parameters

Sine type:

Time (t):

Amplitude:

Bias:

Frequency (rad/sec):

Phase (rad):

Sample time:

Interpret vector parameters as 1-D

## Appendix B: Coding for Piezoelectric and Magnetostrictive Values

```
% 1 kHz and above freq is not suitable for piezo. Output voltage is
very
% small

m = 8.4 * 10^-3 ; %must in gram
b = 0.154 ; %smaller better
k = 2.5 * 10^4 ; %smaller better
Cp = 1.89 * 10^-8 ; %smaller better
a = 1.52 * 10^-3 ; %stay in this unit
R = 30669.6 ; %bigger better
g = 9.8 ; %double,tripple better

m1 = 1 * 10^-3 ; %less better
b1 = 0.24 ; %less better
k1 = 0.569 * 10^3 ; %less better
L1 = 47.16 * 10^-3; %less better
G1 = 0.1448 ; %need to do more research
%R1 = 198.58 ; %smaller is better
Rload = 180 ; %bigger is better
```

## Appendix C: Coding for Resonance Frequency Graph

```
data=xlsread('data.xlsx');
d1=data(:,1);
d2=data(:,2);
d3=data(:,3);
plot(d1,d2,':b',d1,d3,'-r'),title('Resonance
Frequency'),legend('Piezoelectric','Magnetostrictive');
```

## Appendix D: Datasheet for Piezoelectric



**PRODUCT: PPA-1001**

### PPA-1001: OVERVIEW

The PPA-1001 is a single layer product recommended for energy harvesting and sensing applications. It also exhibits good performance as a resonant actuator. It is not recommended for applications requiring high force output. This product does not have mounting and alignment holes like the other products; but it is the most cost effective option Midé has.

### SPECIFICATIONS

Overview		
Capacitance (nF)	100	
Mass (µg)	2.8	
Full Scale Voltage Range (V)	±120	
Layer Material*	Thickness (mils)	Thickness (mm)
Polyester	2.0	0.05
Copper	1.4	0.08
PET 5H	6.0	0.15
Stainless Steel 304	6.0	0.15
Polyimide	1.0	0.08
<b>Total</b>	<b>18.0</b>	<b>0.46</b>

Information on material properties is provided in Section 5.

\*The layer thicknesses do not perfectly add up to the actual thickness of the product due to the epoxy layers. These epoxy layers can be ignored for finite element analysis however.

Stiffness			
Parameter	Clamp -6	Clamp 0	Clamp 6
Effective Stiffness (N/m)	N/A	432.15	275.32
Effective Mass (µg) Max Peak to Peak	N/A	0.918	0.714
Deflection (µm)	N/A	24.0	20.0

See Section 4.3 for more information on how to use this data to tune your piezo.

### DESCRIPTION

Performance data for the PPA-1001 is summarized in the following tables and plots. Refer to Section 6 for information on how this data was gathered. Please note that this data is to be used only as reference and that there is some variability from unit to unit. Temperature, clamp conditions, drive quality, all can contribute to additional variability. All test data was gathered at room temperature and with the PPA-9001 clamp kit hardware.

### DIMENSIONS

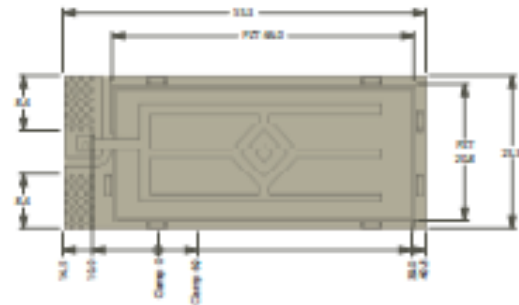


Figure 9: The overall dimensions (mm) for the PPA-1001 are shown. The total thickness is 0.46 mm (18 mils).

## SPECIFICATIONS

Energy Harvesting Data for Middle Clamp Location									
Acceleration Amplitude ( $\mu$ )	Frequency (Hz)	Tip Mass (gram)	RMS Power (mW)	RMS Voltage (V)	RMS Current (mA)	Resistance (k $\Omega$ )	RMS Open Circuit	Peak to Peak Displacement (mm)	Peak to Peak Displacement ( $\mu$ )
0.25	132.0	0.0	0.1	1.1	0.1	17.9	2.1	1.1	0.04
0.50	131.0	0.0	0.2	1.9	0.1	18.8	8.6	1.4	0.05
1.00	131.0	0.0	0.7	3.4	0.2	15.7	6.0	1.6	0.06
2.00	129.0	0.0	2.2	5.4	0.4	13.0	9.9	2.2	0.09
0.25	60.0	1.9	0.1	2.9	0.0	61.0	8.8	1.2	0.05
0.50	60.0	1.8	0.5	3.3	0.2	20.8	6.7	2.1	0.08
1.00	60.0	1.7	1.8	7.1	0.3	28.6	12.2	3.9	0.15
0.25	22.0	22.8	1.4	9.0	0.1	60.4	16.4	5.2	0.21
0.50	22.0	22.8	4.4	17.3	0.3	67.6	26.6	9.3	0.37

Block Force and Static Displacement, 100 volt signal			
Parameter	Clamp -6	Clamp 0	Clamp 6
Block Force Amplitude (N)	N/A	0.20	0.28
Displacement Amplitude (mm)	N/A	0.80	0.74

Dynamic displacement, no added tip mass, +/- 100 volt signal			
Parameter	Clamp -6	Clamp 0	Clamp 6
Resonant Frequency (Hz)	N/A	83.3	98.9
Half Power Bandwidth (Hz)	N/A	5.6	7.8
Q Factor	N/A	14.9	12.7
Peak to Peak Deflection at Resonance (mm)	N/A	19.5	15.9
Quasi Static Peak to Peak Deflection (mm)	N/A	1.4	1.1

Dynamic Displacement, 9.8 tip mass, +/- 100 volt signal			
Parameter	Clamp -6	Clamp 0	Clamp 6
Resonant Frequency (Hz)	N/A	20.5	26.4
Half Power Bandwidth (Hz)	N/A	1.4	1.8
Q Factor	N/A	14.6	14.7
Peak to Peak Deflection at Resonance (mm)	N/A	23.5	19.8
Quasi Static Peak to Peak Deflection (mm)	N/A	1.8	1.8